A Tumor-Protective Role for Human Kallikrein-Related Peptidase 6 in Breast Cancer Mediated by Inhibition of Epithelial-to-Mesenchymal Transition

Georgios Pampalakis,[1] Evangelia Prosnikli,[1] Theodora Agalioti,[2] Antonia Vlahou,[3] Vassilis Zoumpourlis,[4] and Georgia Sotiropoulou[1]

[1]Department of Pharmacy, University of Patras, Rion-Patras, Greece; [2]Biomedical Sciences Research Center "Alexander Fleming", Vari, Attiki, Greece; [3]Foundation of Biomedical Research of the Academy of Athens, and [4]National Hellenic Research Foundation, Athens, Greece

Abstract

Human kallikrein-related peptidase 6 (KLK6) was cloned as a putative class II tumor suppressor based on its inactivated expression in metastatic breast cancer. Here, we investigated the mechanism(s) underlying the silencing of *KLK6* gene in metastatic breast cancer and its putative implications for tumor progression. We present evidence that tumor-specific loss of *KLK6* expression is due to hypermethylation of specific CpGs located in the *KLK6* proximal promoter. Methylation-dependent binding of methyl CpG-binding protein 2 and the formation of repressive chromatin mediated by localized histone deacetylation are critical components of *KLK6* silencing in breast tumors. Re-expression of KLK6 in nonexpressing MDA-MB-231 breast tumor cells by stable cDNA transfection resulted in marked reversal of their malignant phenotype, manifested by lower proliferation rates and saturation density, marked inhibition of anchorage-independent growth, reduced cell motility, and their dramatically reduced ability to form tumors when implanted in severe combined immunodeficiency mice. Interestingly, inhibition of tumor growth was observed at physiologic concentrations of KLK6, but not when KLK6 was highly overexpressed, as observed in a subset of breast tumors. Differential proteomic profiling revealed that KLK6 re-expression results in significant down-regulation of vimentin which represents an established marker of epithelial-to-mesenchymal transition of tumor cells and in concomitant up-regulation of calreticulin and epithelial markers cytokeratin 8 and 19, indicating that KLK6 may play a protective role against tumor progression that is likely mediated by inhibition of epithelial-to-mesenchymal transition. We suggest that KLK6 is an epigenetically regulated tumor suppressor in human breast cancer and provide ways of pharmacologic modulation. [Cancer Res 2009;69(9):3779–87]

Introduction

The cDNA encoding kallikrein-related peptidase 6 (KLK6) was originally identified by mRNA differential display as being highly overexpressed in a primary breast tumor, but completely inactivated in its lung metastasis and the vast majority of metastatic breast cancers (1). Based on this expression pattern, it was suggested that the encoded protein—a novel serine protease—may function to protect against tumor progression and that it is likely deregulated at the transcription level; therefore, it represents a putative class II tumor suppressor (1). However, the putative function(s) of KLK6 in cancer are yet to be elucidated. Remarkably, aberrant expression of *KLK6* gene has been implicated in Alzheimer's and Parkinson's disease (2). In addition, KLK6 is involved in enhanced proteolysis of myelin basic protein associated with multiple sclerosis and central nervous system inflammation (3–5); therefore, it represents a potential therapeutic target for pharmacologic intervention.

At the protein level, the enzymatic activity of KLK6 is controlled by a self-regulatory mechanism (6) that is further supported by the crystal structures of the KLK6 zymogen (7) and mature enzyme (3). The transcription and tissue-specific expression of *KLK6* are likely regulated by multiple mechanism(s) that include alternative splicing of coding exons and utilization of alternative intronic promoters (P2 and P3), in addition to the 5′ upstream promoter (P1) that encodes the classic transcript (8, 9).

Here, we investigated the mechanism(s) underlying the aberrant expression of *KLK6* in breast cancer cells and its putative implications for tumor progression. Our results provide direct molecular evidence for the functional significance of DNA methylation and chromatin structure with respect to the inactivation of *KLK6* expression in metastatic breast cancer. Epigenetic silencing of *KLK6* suggested a tumor suppressor role for the encoded protein. Consistently, we show for the first time that re-expression of KLK6 in the highly tumorigenic MDA-MB-231 breast tumor cell line at concentrations similar to those observed in normal mammary epithelial cells and tissues results in slower proliferation rates, significantly decreased *in vitro* tumorigenicity, and *in vivo* orthotopic tumor formation in severe combined immunodeficiency (SCID) mice. Differential proteomic profiling revealed that KLK6 reactivation results in remarkable down-regulation of vimentin with concomitant up-regulation of epithelial markers and other proteins associated with tumor reversion. Taken together, our data show for the first time that KLK6 exerts a protective role against breast cancer progression that is likely mediated by inhibition of epithelial-to-mesenchymal transition.

Materials and Methods

Materials. Synthetic oligonucleotides were purchased from MWG-BIOTECH, 5-aza-2′-deoxycytidine (5-aza-dC) and trichostatin A (TSA) were from Sigma, [α-^{32}P]dCTP from Amersham, and antibodies were from Santa Cruz Biotechnology. Anti–methyl CpG-binding protein 2 (MeCP2) antibody was from Abcam and anti–acetylated histone 4 was from Upstate.

Note: Supplementary data for this article are available at Cancer Research Online (http://cancerres.aacrjournals.org/).

Requests for reprints: Georgia Sotiropoulou, Department of Pharmacy, University of Patras, Rion-Patras 26500, Greece. Phone: 30-2610-969939; Fax: 30-2610-969940; E-mail: gdsotiro@upatras.gr.

doi:10.1158/0008-5472.CAN-08-1976

Cell culture and treatments. Cell lines were obtained from American Type Culture Collection and maintained in RPMI supplemented with 10% fetal bovine serum (Life Technologies). Human mammary epithelial cells (HMEC) were obtained from Clonetics and maintained in MEGM (Clonetics). For treatments, cells were seeded in 100 mm dishes and grown for 24 h to reach 20% to 30% confluence. Then, 5-aza-dC was added to final concentrations of 50 or 100 μmol/L and cells were incubated for 48 h followed by another 48 h in fresh medium and finally collected for extraction of total cellular RNA using RNeasy (Qiagen). TSA was added to final concentrations of 50, 100, or 200 nmol/L.

Cytotoxicity assay. Cells (7×10^4) were plated on 24-well plates with 1 mL medium and allowed to adhere for 24 h in order to reach 20% to 30% confluence. 5-aza-dC was added at various concentrations and cells were incubated for another 72 h. Then, 100 μL of 5 mg/mL of 3-(4,5-dimethylthiazol-2-yl)-2,5-diphenyltetrazolium bromide (MTT) solution was added and cells were further incubated for 2 h. Medium was removed, the insoluble formazan crystals were dissolved in 1 mL of 100% DMSO, and absorbance was measured at 570 nm. Background controls included medium incubated with MTT.

RNA extraction and reverse transcription-PCR. RNA was extracted with RNeasy and treated with DNase I (Qiagen). Reverse transcription was carried out with Sensiscript (Qiagen) using 2 μg of total RNA and cDNAs were PCR-amplified with gene-specific primers: KLK6S (5′-GGAGGAATTC-CAGCAGGAGCGGCCATG-3′) and KLK6AS (5′-TGTCTCGAGTCAGGGT-CACTTGGCCTG-3′) for *KLK6*, VIMS (5′-GGCTCAGATTCAGGAACAGC-3′) and VIMAS (5′-CTGAATCTCATCCTGCAGGC-3′) for vimentin, ECADS (5′-TGAAGGTGACAGAGCCTCTGGAT-3′) and ECADAS (5′-TGGGTGAA-TTCGGGCTTGTT-3′) for E-cadherin, and ACTINS (5′-ACAATGAGCTG-CGTGTGGCT-3′) and ACTINAS (5′-TCTCCTTAATGTCACGCACGA-3′) for β-actin.

Genomic bisulfite sequencing. Genomic DNA was extracted with GeneElute (Sigma). To convert unmethylated cytosines to uracils, 1 μg of genomic DNA was treated with bisulfite using CpGenome (Intergen) and recovered in 30 μL of TE buffer. Bisulfite-treated DNAs were amplified by PCR with methylation-independent primers: 5′-GTTAGAGATTGTAAAG-GAGGATTGT-3′ and 5′-CACACCTACCCATAAATCCCTCTAT-3′. PCR products were cloned into pCR4-TOPO (Invitrogen). Multiple clones were isolated and sequenced.

Chromatin immunoprecipitation. Cells were grown to 80% to 100% confluence. Chromatin was crosslinked with 1% formaldehyde for varying time intervals as described (10). DNA was purified and dissolved in 100 μL of TE. The *KLK6* (−259, +120) sequence was amplified by hot PCR using 5 μL of DNA template purified after chromatin immunoprecipitation (ChIP), 30 pmol of *KLK6*-specific primers: 5′-ATGGAAGATCTCTCCCCTCCATGGC-CAGG-3′ (forward) and 5′-GAGACAGCTACAGCGTGTGTCACC-3′ (reverse), 200 μmol/L of deoxynucleotide triphosphates, 0.1 μL of [α-^{32}P]dCTP, and 1 unit per reaction of Taq Polymerase (Promega). PCR products were resolved on 6% acrylamide gels and visualized with Phosphor Imager (Molecular Dynamics SSD).

Western blot. Cell lysates (40 μg) were resolved by 12% SDS-PAGE and blotted on a polyvinylidene difluoride membrane (Millipore) that was blocked and incubated with appropriate antibodies (1:1,000). Then, it was washed in PBS-T and incubated with horseradish peroxidase–labeled secondary antibody (1:4,000). Specific immunoreactive bands were detected with enhanced chemiluminescence (Pierce).

Expression constructs. The cDNA encoding preproKLK6 was PCR-amplified from full-length *KLK6* cDNA using primers KLK6S and KLK6AS and cloned into pcDNA3.1(+) (Invitrogen). Plasmid DNAs were purified and confirmed by DNA sequencing.

Stable transfections. MDA-MB-231 cells were grown in 100 mm dishes for 24 h and transfected with Polyfect (Qiagen). Polyfect was removed after 48 h and fresh medium containing 0.5 mg/mL of G418 was added for selection. Individual colonies of stably-transfected cells were picked after 3 weeks. The concentration of KLK6 in serum-free conditioned media was measured by ELISA (11).

Growth curves and soft agar assay. For growth curves, 2.7×10^4 cells were seeded into six-well plates and counted on days 1, 3, 5, 7, and 9. Determination of population doubling time was performed by plotting ln(cell number) versus time (days) for the logarithmic phase of growth and fitting the data according to the least squares mean method. A soft agar assay was performed as previously described (12). Colonies were stained with 1 mg/mL of MTT for 24 h and counted in double-blinded experiments. Results and corresponding SDs were derived from three independent experiments.

Wound scratch assay. Cells (4×10^5) were seeded in six-well plates and left to grow to confluence. The monolayer was wounded by scraping a line across the well with a sterile blue pipette tip. Cells were washed with PBS and refreshed with RPMI supplemented with 10% fetal bovine serum. After 24 h, plates were photographed at the marked spots.

Proteomic profiling. Cell lysates were prepared from 10^8 cells and resolved by two-dimensional PAGE. Differentially expressed proteins were identified by mass spectrometry. Lysates were analyzed three separate times. Results were confirmed in two independent experiments.

***In vivo* tumor formation.** Cells (2×10^6) were resuspended in 200 μL of PBS and injected bilaterally into the mammary fat-pad of 6-week-old female SCID mice. Mice were examined on alternate days for the presence of palpable tumors. Tumors were allowed to grow for the indicated times and tumor sizes were measured double-blinded. Then, mice were sacrificed and photographed. Expression of KLK6 in dissected tumor specimens was verified by reverse transcription-PCR (RT-PCR) and Western blot (data not shown). Tumor volumes were calculated using the formula: 1/2 × height × width × length. Experiments were conducted according to the guidelines of our institutions for animal handling.

Results

Aberrant expression of *KLK6* gene in breast cancer. Differential expression of *KLK6* in normal and tumor mammary cell lines was confirmed by semiquantitative RT-PCR. Protein concentrations were measured in cell culture supernatants by a sensitive and specific ELISA (11). For investigation of the molecular mechanism(s) underlying the aberrant *KLK6* expression patterns observed in breast cancer, a panel of cell lines was selected which included HMECs normal human mammary epithelial cell strain (12 μg/L KLK6 protein, +*KLK6* mRNA), T47D (0.06 μg/L KLK6, +/−*KLK6* mRNA) and MDA-MB-231 (0.00 μg/L KLK6, −*KLK6* mRNA), two nonexpressing tumor cell lines, and MDA-MB-468, a breast tumor cell line that highly overexpresses *KLK6* (400 μg/L KLK6, +++*KLK6* mRNA).

Reactivation of *KLK6* expression. Treatment of MDA-MB-231 and T47D breast tumor cell lines with 5-aza-dC, an inhibitor of DNA methyltransferases, resulted in significant induction of *KLK6* expression (Fig. 1*A*), implicating genomic DNA methylation in *KLK6* silencing. As depicted in Fig. 1*B*, TSA that acts as a potent inhibitor of histone deacetylases (HDAC) up-regulated *KLK6* expression dose-dependently in MDA-MB-231 although to a lesser extent than 5-aza-dC. No change in *KLK6* expression was observed upon treatment of T47D cells with TSA. These findings indicated that epigenetic mechanisms likely underlie the inactivation of *KLK6* in breast cancer cells and pointed to the predominant role of DNA methylation over histone deacetylation in *KLK6* silencing. Reactivation of *KLK6* expression was also detected in various breast cancer cell lines using lower concentrations of 5-aza-dC (3–10 μmol/L) for a longer period of time (6 days; data not shown). No signs of severe cytotoxicity were observed in the presence of 100 μmol/L of 5-aza-dC, indicating that reactivation of *KLK6* expression is most likely associated with DNA demethylation, although it cannot be excluded that the observed up-regulation might also be due to a secondary effect involving cytotoxic mechanisms. As depicted in Fig. 1*C*, even after 3 days of treatment

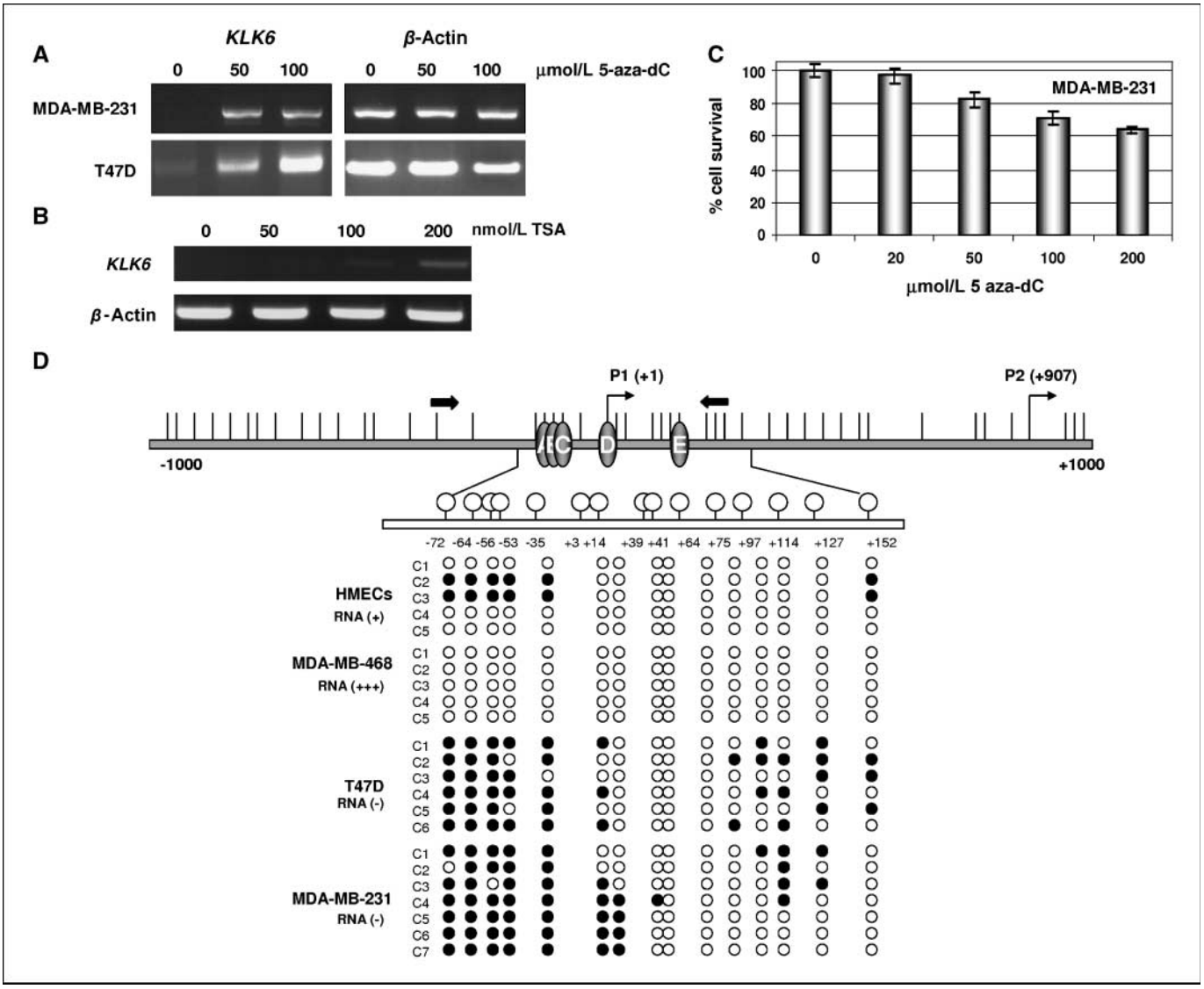

Figure 1. *KLK6* expression is induced in breast cancer cell lines by DNA methyltransferase and HDAC inhibitors. Identification of methylated CpG dinucleotides in the 5′ upstream sequence of *KLK6*. *A,* MDA-MB-231 and T47D cells treated with 5-aza-dC. *B,* MDA-MB-231 cells treated with TSA. Gene expression was analyzed by RT-PCR. *C,* no signs of severe cytotoxicity were observed after incubating MDA-MB-231 cells with 5-aza-dC for 72 h. *D,* methylation of CpGs was analyzed by genomic bisulfite sequencing of HMECs, MDA-MB-468, T47D, and MDA-MB-231 cells. Schematic representation of CpGs (*thin vertical lines*). Each row represents one sequenced allele. *Arrows,* transcription start sites of P1 (+1) and P2 (+907) alternative *KLK6* promoters. Positions of CpGs analyzed here (*lollipops*) are given on the horizontal open bar. *Ovals,* putative Sp1 binding sites identified by SignalScan (http://thr.cit.nih.gov/molbio/signal). Each circle represents a CpG dinucleotide: methylated (●) or unmethylated (○). Numbering was based on GenBank sequence AY804248 of *KLK6* P1 promoter.

with 200 μmol/L of 5-aza-dC, ~65% of MDA-MB-231 cells were viable. It should be noted that similar 5-aza-dC concentrations were used previously for the induction of genomic DNA hypomethylation in breast cancer cell lines (13).

Identification of methylated CpG dinucleotides. Biocomputational analysis using CpGplot (European Bioinformatics Institute) identified no typical CpG islands in 12 kb of *KLK6* genomic sequence (GenBank: AF149289). Interestingly though, recent data suggested that gene silencing by DNA methylation does not necessarily require a CpG island (14). Therefore, we searched for methylated cytosines at CpG sites, in association with inactivated *KLK6* expression. The 5′ upstream *KLK6* (−105, +164) sequence schematically shown in Fig. 1*D*, which flanks the transcriptional start site of the P1 promoter (15), was selected for bisulfite sequencing analysis based on its high C+G content of 68% and high density of CpG dinucleotides, i.e., 15 CpGs in a region of 269 bp, and the observed/expected ratio of 0.48. Using methylation-independent primers, PCR amplification was carried out to generate a 319 bp amplicon that contained the above CpG dinucleotides. For each cell line, multiple PCR amplicons were cloned and sequenced. Based on the obtained sequences, shown in Fig. 1*D*, methylated cytosines occurred at positions −72, −64, −56, −53, −35, +3, +14, +97, +114, and +127. Interestingly, the identified CpGs were completely unmethylated in the MDA-MB-468 cell line that overexpresses *KLK6*. On the other hand, in MDA-MB-231 and T47D cell lines that are characterized by complete loss of *KLK6* expression, the identified cytosines were fully methylated. Analysis of a large number of mammary tumor cell lines revealed a direct correlation of *KLK6* mRNA levels with the extent of methylation of the identified CpGs (data not shown; Supplementary Fig. S1).

As shown in Fig. 1*D*, HMECs that express relatively low *KLK6* mRNA and protein levels were methylated to much lower levels and contained a heterogeneous mixture of methylated and unmethylated alleles. This result indicates that tissue-specific expression of *KLK6* may in part be determined by the extent of genomic DNA methylation, as has been well-documented for maspin (16). The methylation status of the identified CpGs was analyzed in tissue specimens obtained from patients diagnosed with breast cancer and normal controls. Correspondingly, similar methylation patterns of the identified CpGs as those described above for tumor cell lines and normal mammary cell strains were detected in clinical tissue specimens (Supplementary Fig. S1).

Methylated CpGs are localized in the *KLK6* proximal promoter. Using ChIP assay, we showed that components of the basal transcription machinery, i.e., TATA-binding protein and RNA *Pol*II, are bound to the *KLK6* sequence from −259 to +120 in the MDA-MB-468 *KLK6*-expressing cells but not in the MDA-MB-231 nonexpressing cells (Fig. 2*A*). For optimization of crosslinking conditions, increasing chromatin-DNA crosslinking times were tested (*top*). Optimal crosslinking was achieved in 45 min, whereas shorter incubations (15 and 30 min) led to DNA-protein crosslinks that were not stable during subsequent incubation with proteinase K and yielded no detectable PCR products. Prolongation of incubation with formaldehyde may result in changes in the tertiary structure of proteins with implications for antibody recognition. It was found that treatment of MDA-MB-231 cells with TSA causes recruitment of the basal transcription machinery to the *KLK6* promoter probably due to acetylation of core histones (Fig. 2*A*) and activates transcription and *KLK6* expression as shown in Fig. 1*B*, thus, implicating suppressive chromatin structure in the silencing of *KLK6* in breast cancer cells.

Methylation-dependent binding of MeCP2 mediates the repression of *KLK6* expression in breast cancer cells. To investigate the recruitment events associated with constitutive and inducible *KLK6* transcription in breast cancer cells, we performed a series of ChIP experiments using chromatin prepared from MDA-MB-468 and MDA-MB-231 cells and antibodies against the acetylated tail of histone H4, MeCP2, and histone acetyltransferases, CBP and GCN5. Figure 2*B* and *C* shows that constitutive and inducible expression of *KLK6* positively correlates with histone H4 tail acetylation. *KLK6* upstream sequences containing the identified methylated CpG dinucleotides are enriched in MDA-MB-468 chromatin that was immunoprecipitated with the α-acetyl histone H4 compared with MDA-MB-231 chromatin (Fig. 2*B*). Additionally, both TSA and 5-aza-dC treatment resulted in increased histone H4 tail acetylation in the *KLK6* promoter in MDA-MB-231 (Fig. 2*B*) and in T47D cells (Fig. 2*C*), respectively. This enhanced histone H4 acetylation was accompanied by the presence of the CBP coactivator and TATA-binding protein basal transcription factor to *KLK6* promoter in MDA-MB-468 and TSA-treated MDA-MB-231 cells. CBP is a histone acetyltransferase that, along with GCN5, could be responsible for the enhanced histone H4 acetylation that we observed when the gene is expressed. Finally, we observed an inverse correlation between binding of the methyl-binding protein MeCP2 to *KLK6* upstream sequences and expression of *KLK6*. MeCP2 binding is not detected in *KLK6* upstream sequences in MDA-MB-468–expressing cells whereas MeCP2 departs in TSA-treated MDA-MB-231 and 5-aza-dC–treated T47D cells, respectively. Taken together, these data show that TSA and 5-aza-dC treatment of cancer cells induce *KLK6* gene transcription and that this induction correlates with departure of MeCP2 repressor from the *KLK6* promoter.

Selection of *KLK6*-transfected cells. The epigenetic silencing of *KLK6* in metastatic tumor cells that was described here points to a putative tumor suppressor function of the encoded protein. Although loss of function of tumor suppressor genes through

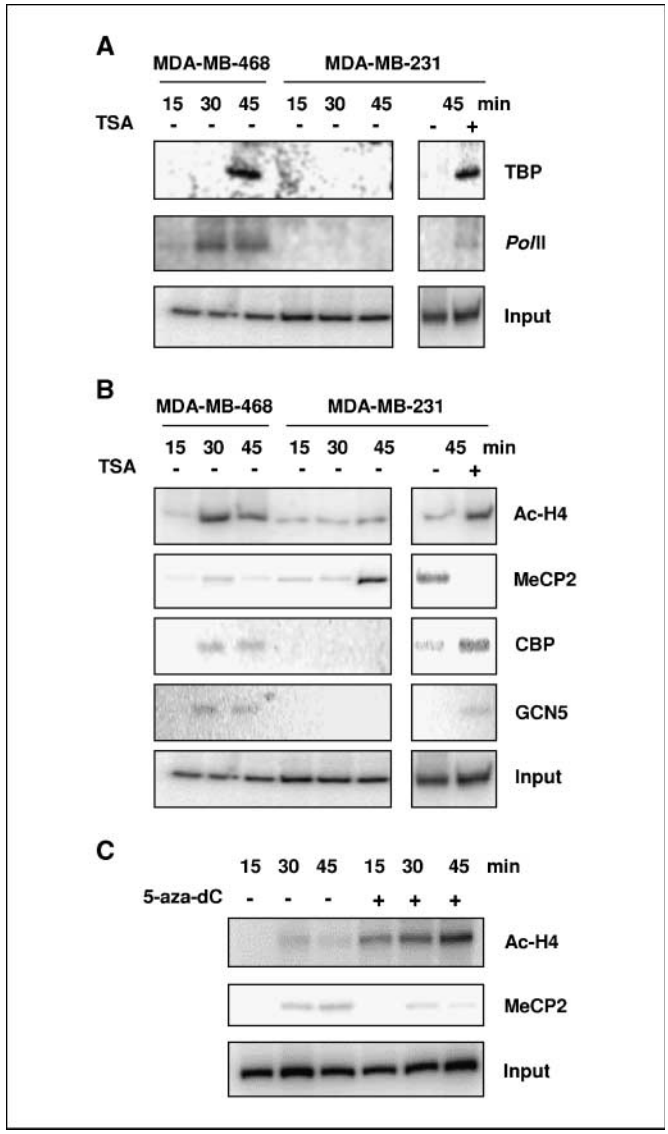

Figure 2. Repression of KLK6 expression in breast cancer cells is mediated by methylation-dependent binding of MeCP2. Recruitment events associated with constitutive and inducible KLK6 transcription in MDA-MB-468 and MDA-MB-231 breast cancer cells, respectively, were analyzed by ChIP using antibodies against histone H4 acetylated tail, MeCP2, and histone acetyltransferases CBP and GCN5. *A,* histone deacetylation upon treatment of MDA-MB-231 cells with 200 nmol/L of TSA reactivated *KLK6* transcription by recruiting proteins from the basal transcription machinery on *KLK6* chromatin. Crosslinked chromatin prepared from MDA-MB-468 and MDA-MB-231 cells was immunoprecipitated with specific antibodies (*right*). Increasing crosslinking times (*top*). Immunoprecipitates were subjected to PCR using a primer pair spanning the region containing the methylated CpGs (Fig. 1*D*). Aliquots of chromatin taken before immunoprecipitation were used as "Input" controls. *B,* recruitment of MeCP2, histone acetyltransferases, and acetylation status of H4 at the *KLK6* CpG-containing chromatin was shown by ChIP. *In vivo* binding of Ac-H4, MeCP2, CBP, and GCN5 was examined in *KLK6*-positive MDA-MB-468 and in *KLK6*-negative MDA-MB-231 cells (*left*). *KLK6* chromatin is enriched in Ac-H4 upon HDAC inhibition with TSA (*right*). *C,* release of the MeCP2 repressor and marked increase of Ac-H4 binding to *KLK6* chromatin following treatment of T47D cells with 100 μmol/L of 5-aza-dC.

genetic mutations is a hallmark in human cancers, hypermethylation of genomic DNA that usually, but not exclusively, occurs in promoter sequences provides a frequent mechanism of transcriptional silencing and functional disruption of known tumor suppressor genes in cancer cells (13, 17–22). To test whether inactivation of *KLK6* expression by genomic DNA hypermethylation, and thereafter, lack of KLK6 function provides a growth advantage to metastatic breast tumor cells, the MDA-MB-231 cell line was stably transfected with an expression construct that directs the synthesis of preproKLK6. Stably transfected cells were selected based on the concentrations of secreted KLK6 protein determined by ELISA (Table 1) and established in cultures.

Stable expression of *KLK6* reduces proliferation rates, motility, and anchorage-independent growth of MDA-MB-231 cells. The growth rates of parental and mock-transfected cells were compared with that of *KLK6*-transfected cells. As shown in Fig. 3*A* and Table 1, expression of KLK6 protein at physiologic levels (clones: C6wt, C11wt, and C12wt) resulted in reduced proliferation rates of MDA-MB-231 cells. Interestingly, *KLK6*-transfected cells grew to lower saturation densities than parental or mock controls (Table 1). Based on previous observations that a small subset of primary breast tumors highly overexpress (e.g., 50-fold to 100-fold higher than normal) *KLK6* mRNA and protein (1), a *KLK6*-overexpressing clone (C5wt) was selected that was found to proliferate with exactly the same rate and reached similar saturation density as parental cells (Table 1). The motility of parental, mock-transfected, and *KLK6*-transfected MDA-MB-231 cells (Fig. 3*B*) was assessed with the wound scratch (healing) assay (23). Parental and mock-transfected cells were capable of closing the wound almost completely within 24 hours, whereas cells of *KLK6*-expressing MDA-MB-231 clones were less motile and showed significantly slower rates of wound-healing (Fig. 3*B*). Finally, the effect of *KLK6* expression on the tumorigenicity of MDA-MB-231 was assessed *in vitro* by soft agar assay (12). As shown in Fig. 3*C*, parental and mock controls yielded numerous colonies in a period of 3 weeks, whereas a very small number of smaller-sized colonies were obtained for *KLK6*-expressing clones C6wt, C12wt, and C11wt (data not shown), indicating that KLK6 protein acts to inhibit the anchorage-independent growth of tumor cells. The growth of C5wt cells in soft agar, although significant, was suppressed to a lesser extent (Fig. 3*C*). Taken together, our data shows that KLK6 reverses the malignant phenotype of MDA-MB-231 cells and supports the idea that KLK6 might play a tumor suppressor role in breast cancer.

Identification of molecular alterations caused by KLK6. Differential proteomic profiling of parental, mock-transfected, and *KLK6*-transfected MDA-MB-231 cells was applied to the identification of potential substrates for KLK6. Figure 4*A* shows a representative pattern of two-dimensional electrophoresis of cell lysates. Proteins displaying differential expression between parental (data not shown), mock-transfected, and *KLK6*-transfected C12wt cells are shown (Fig. 4*A*; Supplementary Table S1). Unexpectedly, we found that vimentin, a mesenchymal marker, was dramatically down-regulated in *KLK6* transfectants as compared with mock and parental controls (mean, 9-fold reduction). Western blot analysis confirmed that vimentin levels are significantly decreased in *KLK6* transfectants (Fig. 4*B*). Because RT-PCR showed no change in vimentin mRNA, reduction of vimentin concentration must occur posttranslationally. Down-regulation of vimentin upon expression of KLK6 suggests a possible "mesenchymal-to-epithelial–like" (MET-like) transition that would be compatible with a tumor suppressor role (24). Interestingly, significant up-regulation of the epithelial markers cytokeratin 8 (3-fold) and cytokeratin 19 (10-fold), as well as of calreticulin (3-fold), was detected in *KLK6*-transfected cells. However, expression of E-cadherin, which is an established epithelial marker (24), was not induced in *KLK6* transfectants, as shown by RT-PCR and Western blot (Fig. 4*B*).

KLK6 inhibits tumor formation in SCID mice. Parental MDA-MB-231 and mock-transfected cells grew to palpable tumors 6 to 7 weeks after implantation into the mammary fat-pads of SCID mice (Table 2; Supplementary Fig. S2, *top*). Tumors developed rapidly and exceeded a volume of 1,000 mm^3 after 4 months. In one case, the tumor exceeded a volume of 6,000 mm^3. In contrast, *KLK6*-transfected cells showed significant inhibition of tumor growth *in vivo*. More specifically, clones C11wt and C12wt did not develop tumors even after 4 months following implantation, whereas clone C6wt grew tumors, although with a significantly delayed onset and a slower proliferation rate when compared with parental or mock controls (Table 2; Supplementary Fig. S2, *bottom*). The tumor volume was significantly smaller for C6wt cells (mean, 20 mm^3; day 77) when compared with parental and mock controls (mean, 200 mm^3; day 77; Table 2). Taken together, these results indicate that re-expression of KLK6 at physiologic concentrations inhibits tumor formation *in vivo* and support a tumor suppressor role for this protein. Interestingly, when KLK6 is produced at abnormally high levels, e.g., >100 and 400 μg/L, as in C5wt and MDA-MB-468 tumor cells, respectively, no inhibition of tumor growth was observed. We found that C5wt cells form tumors with the same efficiency as parental and mock controls in terms of onset, growth rates, frequency, and tumor volume at the end point (Table 2;

Table 1. *In vitro* growth characteristics of MDA-MB-231 parental, mock-transfected, and *KLK6*-transfected clones stably expressing varying concentrations of KLK6

Cell line	KLK6 (μg/L)	PDT (h)	Saturation density ($10^6/cm^2$)
Parental	ND	33.63 ± 1.00	1.05 ± 0.14
Mock	ND	28.90 ± 0.60	1.06 ± 0.17
C5wt	>100	33.90 ± 0.80	1.02 ± 0.20
C6wt	2.5	41.35 ± 2.47	0.64 ± 0.10
C11wt	1.0	43.63 ± 1.11	0.55 ± 0.05
C12wt	28	40.13 ± 0.98	0.75 ± 0.15

Abbreviations: ND, not detected; PDT, population doubling time.

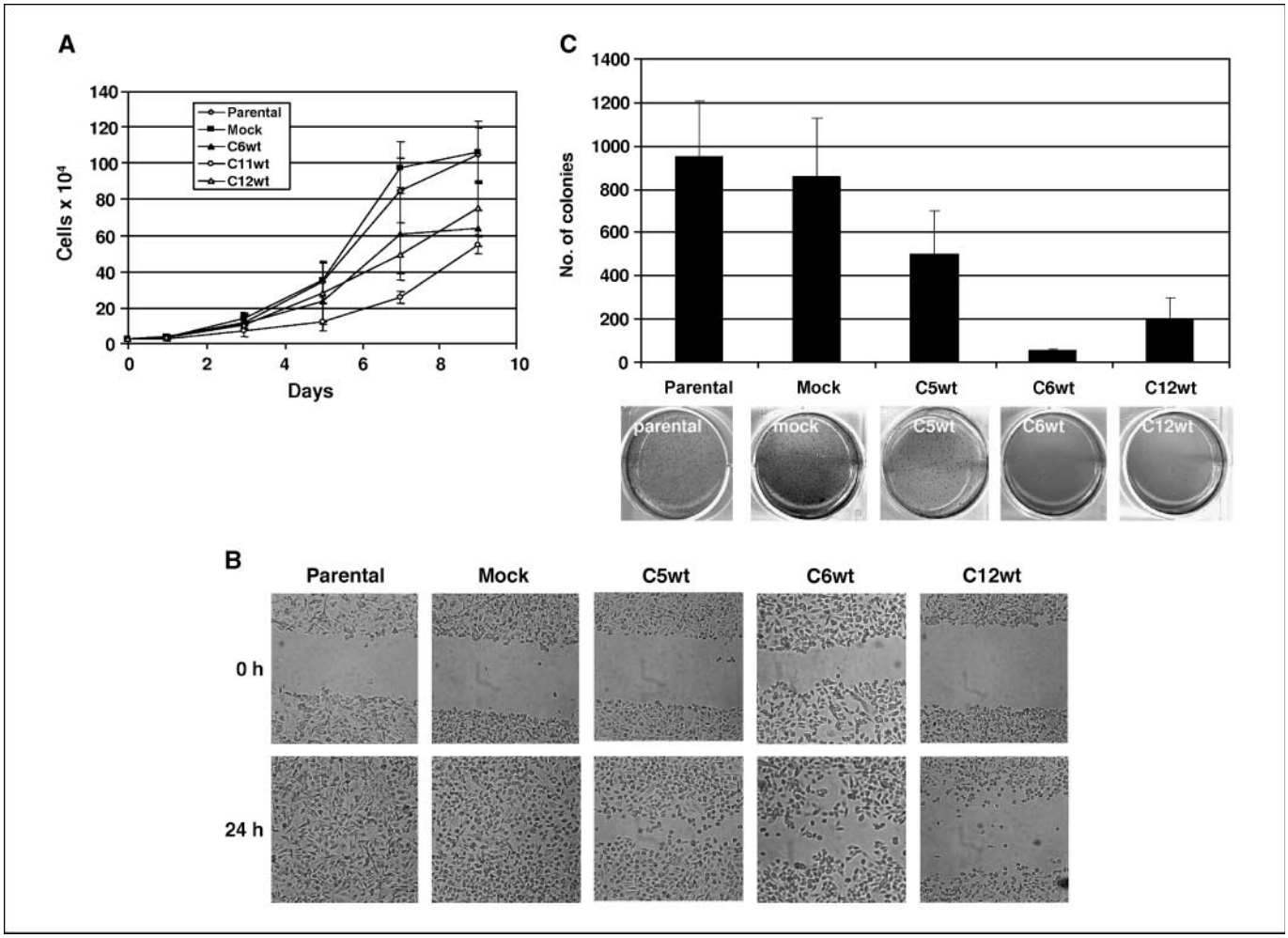

Figure 3. Re-expression of KLK6 by stable cDNA transfection results in the suppression of the malignant phenotype of MDA-MB-231 breast tumor cells. *A,* KLK6 reduces the proliferation rates and saturation density of MDA-MB-231 cells. *B,* KLK6 reduces the motility of MDA-MB-231 cells as assessed by the wound-healing assay. A representative experiment of at least three replicates. *C,* transfection of *KLK6* cDNA in MDA-MB-231 remarkably suppressed anchorage-independent growth of MDA-MB-231 cells. Inhibition of anchorage-independent growth was not as prominent for C5wt cells that highly overexpress KLK6. Results and corresponding SDs were derived from three independent experiments.

Supplementary Fig. S2). Notably, in two C5wt-injected sites, the final tumor volume exceeded 6,000 mm^3, as also observed for parental MDA-MB-231 cells in one case. Similarly, the onset of MDA-MB-468 tumor growth in SCID mice was observed in only 3 weeks and tumors continued to grow very efficiently (in six of six sites injected; data not shown).

Discussion

Kallikrein-related peptidases participate in proteolytic cascades that regulate important physiologic and pathophysiologic processes (25). Aberrant expression of KLK6 has been associated with human breast and ovarian cancers, although the molecular mechanisms underlying this dysregulation have not been described. Here, we show that 5-aza-dC induces *KLK6* expression in *KLK6*-negative breast cancer cell lines. TSA reactivates *KLK6* only in MDA-MB-231 cells. Although *KLK6* lacks a typical CpG island, the methylation status of distinct CpG dinucleotides located in *KLK6* proximal promoter correlated with *KLK6* expression. We found that tumor-specific loss of *KLK6* expression results from hypermethylation of these CpGs, whereas their complete demethylation is associated with the constitutive *KLK6* expression observed in a subset of breast tumors.

Recruitment events to *KLK6* proximal promoter were studied by ChIP in MDA-MB-468 cells, in which *KLK6* expression is constitutive, and during induction of *KLK6* expression in TSA-treated MDA-MB-231 and in 5-aza-dC–treated T47D cells. It was shown that the mechanisms of constitutive and inducible transcription of *KLK6* are likely different and that CpG methylation–mediated *KLK6* silencing in cancer cells is associated with the formation of transcriptional repression complexes, e.g., recruitment of MeCP2 and localized deacetylation of histone H4. The identification of the MeCP2 repressor in *KLK6* chromatin is compatible with the lack of CpG islands because MeCP2-mediated repression does not require a CpG island. Interestingly, MeCP2 has been shown to repress transcription by binding even to a single methylCpG (26). Methylated DNA and MeCP2 recruit corepressor complexes that mediate repression through deacetylation of core histones (27), with consequent compaction of DNA into the heterochromatin. MeCP2 can displace histone H1 from preassembled chromatin that contains methylCpG and recruits HDACs to suppress gene expression (27–30). Our data shows that 5-aza-dC

treatment of breast cancer cells induces *KLK6* transcription and that this induction correlates with the departure of the MeCP2 transcriptional repressor from the *KLK6* promoter. Surprisingly, activation of *KLK6* by TSA also forces MeCP2 to vacate the promoter. It could be either that MeCP2 protein binding is incompatible with histone acetylation on this promoter or that TSA may cause site-specific DNA demethylation (31). In conclusion, methylation-dependent binding of MeCP2 and the formation of repressive chromatin inhibit the transcription of *KLK6* by interfering with the recruitment and function of the basal transcription machinery.

Epigenetic silencing of *KLK6* in breast cancer cells suggested that the encoded protein could normally play a tumor suppressor

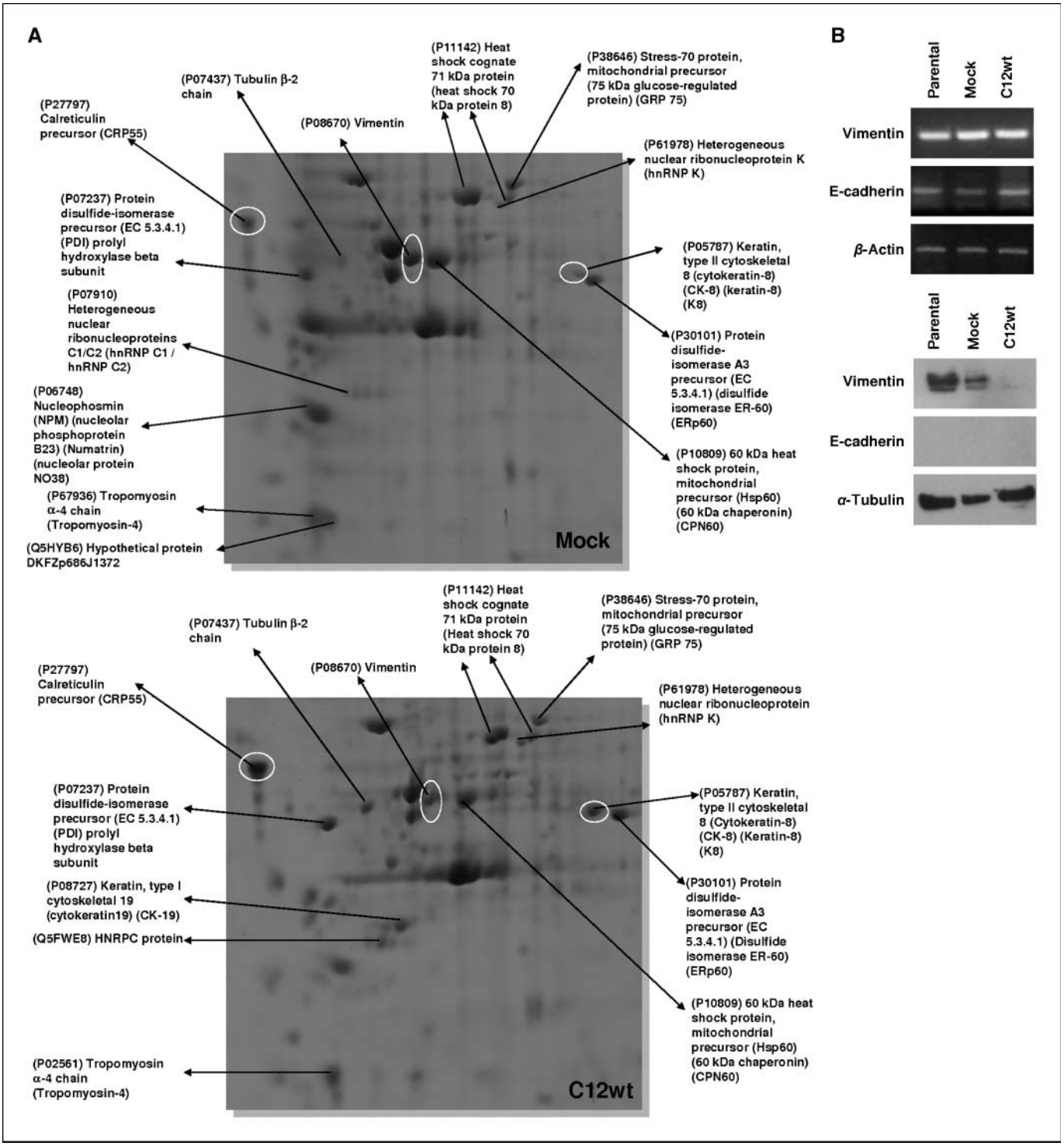

Figure 4. Molecular changes in the intracellular proteome accompanied by reconstitution of KLK6 expression. *A,* lysates from mock and C12wt cells were analyzed by two-dimensional PAGE. *Circles,* differentially expressed proteins (also shown in Supplementary Table S1). *B,* down-regulation of vimentin was confirmed by Western blot analysis, whereas no change in mRNA levels was detected by RT-PCR. Protein and mRNA levels of E-cadherin were not altered.

Table 2. Tumor formation in SCID mice

Cell line	Onset of tumor formation (wk)	No. of sites injected	Sites which developed tumors at 77 d (%)	Size of primary tumors at 77 d (mm^3)	Sites which developed tumors at 96 d (%)	Size of primary tumors at 96 d (mm^3)
Parental	6	15	100	227 ± 68	100	1,357 ± 366
Mock	6–7	16	100	270 ± 100	100	Sacrificed
C5wt	6–7	18	100	292 ± 274	100	1,429 ± 995
C6wt	7–8	18	72	21 ± 13	89	430 ± 122
C11wt	No tumor	10	0	0	0	0
C12wt	No tumor	24	0	0	0	0

role. Therefore, we stably transfected the *KLK6* cDNA into nonexpressing MDA-MB-231 breast tumor cell line and investigated potential effects on the tumor cell phenotype. We found that re-expression of KLK6 at physiologic concentrations, as those found in breast cyst fluid from normal humans, e.g., 1 to 30 μg/L (mean, 10 μg/L; ref. 32), reversed the tumorigenicity of MDA-MB-231 cells *in vitro*. Most importantly, re-expression of KLK6 resulted in the repression of *in vivo* orthotopic tumor formation when MDA-MB-231 cells were implanted in SCID mice, indicating a tumor suppressor role for KLK6 in breast cancer. Notably, in C5wt and MDA-MB-468 tumor cells, in which KLK6 is produced at abnormally high levels, no inhibition of tumor growth was observed. Here, we showed that this constitutive overexpression of *KLK6* in MDA-MB-468 and 21PT (data not shown) primary breast tumor cells is associated with complete demethylation of the identified CpGs. Overexpression of *KLK6* in cancer cells might also result from gene amplification, as reported for a subset of ovarian tumors (33). Possibly, such abnormal tumor-associated overproduction of KLK6 may stimulate tumor growth by activating protease-activated receptor 2 signaling (34), given the fact that both MDA-MB-468 and MDA-MB-231 cells express protease-activated receptor 2 (35). Indeed, it was shown recently that KLK6 can activate protease-activated receptor 2 at very high concentrations (1.6 nmol/L; ref. 34) that are comparable to those produced by C5wt (2.5 nmol/L) and MDA-MB-468 (10 nmol/L). In contrast, in normal HMECs and in *KLK6* transfectants (C6wt, C11wt, and C12wt), the concentration of KLK6 lies in the range 25 to 600 pmol/L. Validation of protease-activated receptor 2 activation in KLK6-overexpressing tumors will be required to confirm this hypothesis. Transient overexpression of KLK6, which was originally observed in 21PT primary breast tumor as compared with its corresponding metastasis (21MT-1; ref. 1), might support tumor growth at the primary site. On the other hand, reactivation of KLK6 expression at normal levels inhibits tumor progression, as shown here, by inducing MET-like tumor reversion.

Indeed, differential proteomic profiling of parental, mock-transfected, and *KLK6*-transfected MDA-MB-231 cells revealed that restoration of KLK6 results in extensive down-regulation of the major mesenchymal marker vimentin that is characteristic of aggressive forms of breast cancer (36), and concomitant up-regulation of epithelial markers such as cytokeratin 8 and cytokeratin 19, and of calreticulin, a protein with a molecular chaperone function and antiangiogenic activity (37). Down-regulation of vimentin is associated with reduced tumor aggressiveness (38). In addition, up-regulation of cytokeratin 8, which is usually not expressed in metastatic breast cancer cells (39), and reduced motility observed in *KLK6*-transfected cells are both compatible with MET-like tumor reversion (24). Therefore, KLK6 likely promotes a MET-like transition, a function that merits further thorough investigation. Vimentin was also markedly repressed in KLK6-overexpressing C5wt and MDA-MB-468 cells. It should be noted, however, that we could not detect a significant up-regulation of E-cadherin that represents the major epithelial marker or "caretaker" of the epithelial phenotype (24). How KLK6 expression results in down-regulation of vimentin is unknown. Direct cleavage of vimentin by KLK6 is unlikely because KLK6 is an extracellular protease. Construction of the KLK6 interactome revealed that KLK6 might act via the transforming growth factor-β1 (TGF-β1) pathway to reduce TGF-β1 levels by degrading the extracellular protein fibronectin (40). Fibronectin increases steady-state mRNA levels of TGF-β1 that is known to up-regulate vimentin and to down-regulate cytokeratin 8 and calreticulin. Indeed, we have shown that TGF-β1 levels reverse-correlate with KLK6 expression in TGF-β1–treated breast tumor cells.[5]

Proteases were considered to act as tumor promoters by degrading components of the extracellular matrix. Accumulating evidence indicates that specific proteases inhibit early tumor growth or/and progression (41). KLK6 has been implicated in the induction of differentiation of colon (42) and squamous cell carcinomas (43), and in the inhibition of angiogenesis (6), compatible with its function as a tumor suppressor.

In summary, it was shown for the first time that KLK6 normally exerts a tumor-protective function against breast cancer that is likely mediated by inhibition of epithelial-to-mesenchymal transition, and that epigenetic mechanisms underlie its loss-of-function in breast tumor cells. Pharmacologic modulation of *KLK6* gene expression described here may be exploited therapeutically.

Disclosure of Potential Conflicts of Interest

No potential conflicts of interest were disclosed.

Acknowledgments

Received 5/31/08; revised 2/14/09; accepted 3/4/09; published OnlineFirst 4/21/09.

Grant support: K. Karatheodoris (C.186) provided by the Research Committee of the University of Patras and PENED2003 (03EΔ430) cofunded by the E.U. European Social Fund (75%) and the Greek Ministry of Development-GSRT (25%).

The costs of publication of this article were defrayed in part by the payment of page charges. This article must therefore be hereby marked *advertisement* in accordance with 18 U.S.C. Section 1734 solely to indicate this fact.

We thank Eleftherios P. Diamandis and Antoninus Soosaipillai for ELISA determinations, Nikos Youroukos for his help with animal experiments, and Evi Lianidou and Vassilis Georgoulias for providing the clinical samples.

[5] Our unpublished data.

References

1. Anisowicz A, Sotiropoulou G, Stenman G, Mok SC, Sager R. A novel protease homolog differentially expressed in breast and ovarian cancer. Mol Med 1996; 2:624–6.
2. Borgoño CA, Diamandis EP. The emerging roles of human tissue kallikreins in cancer. Nat Rev Cancer 2004; 4:876–90.
3. Bernett MJ, Blaber SI, Scarisbrick IA, Dhanarajan P, Thompson SM, Blaber M. Crystal structure and biochemical characterization of human kallikrein 6 reveals that a trypsin-like kallikrein is expressed in the central nervous system. J Biol Chem 2002;277:24562–70.
4. Scarisbrick IA, Blaber SI, Lucchinetti CF, Genain CP, Blaber M, Rodriguez M. Activity of a newly identified serine protease in CNS demyelination. Brain 2002;125: 1283–96.
5. Blaber SI, Ciric B, Christophi GP, et al. Targeting kallikrein 6 proteolysis attenuates CNS inflammatory disease. FASEB J 2004;18:920–2.
6. Bayés A, Tsetsenis T, Ventura S, Vendrell J, Avilés FX, Sotiropoulou G. Human kallikrein 6 activity is regulated via an autoproteolytic mechanism of activation inactivation. Biol Chem 2004;385:517–24.
7. Gomis-Ruth FX, Bayés A, Sotiropoulou G, et al. The structure of human prokallikrein 6 reveals a novel activation mechanism for the kallikrein family. J Biol Chem 2002;277:27273–81.
8. Pampalakis G, Kurlender L, Diamandis EP, Sotiropoulou G. Cloning and characterization of novel isoforms of the human kallikrein 6 gene. Biochem Biophys Res Commun 2004;320:54–61.
9. Christophi GP, Isackson PJ, Blaber S, Blaber M, Rodriguez M, Scarisbrick IA. Distinct promoters regulate tissue-specific and differential expression of kallikrein 6 in CNS demyelinating disease. J Neurochem 2004;91:1439–49.
10. Agalioti T, Chen G, Thanos D. Deciphering the transcriptional histone acetylation code for a human gene. Cell 2002;111:381–92.
11. Diamandis EP, Yousef GM, Soosaipillai AR, et al. Immunofluorometric assay of human kallikrein 6 (zyme/protease M/neurosin) and preliminary clinical applications. Clin Biochem 2000;33:369–75.
12. Goyal J, Smith KM, Cowan JM, Wazer DE, Lee SW, Band V. The role for NES1 serine protease as a novel tumor suppressor. Cancer Res 1998;58:4782–6.
13. Li B, Goyal J, Dhar S, et al. CpG methylation as a basis for breast tumor-specific loss of NES1/kallikrein 10 expression. Cancer Res 2001;61:8014–21.
14. Jones PA, Baylin SB. The fundamental role of epigenetic events in cancer. Nat Rev Genet 2002;3:415–28.
15. Pampalakis G, Sotiropoulou G. Multiple mechanisms underlie the aberrant expression of the human kallikrein 6 gene in breast cancer. Biol Chem 2006;387:773–82.
16. Futscher BW, Oshiro MM, Wozniak RJ, et al. Role for DNA methylation in the control of cell type specific maspin expression. Nat Genet 2002;31:175–9.
17. Herman JG, Latif F, Weng Y, et al. Silencing of the VHL tumor-suppressor gene by DNA methylation in renal carcinoma. Proc Natl Acad Sci U S A 1994; 91:9700–4.
18. Merlo A, Herman JG, Mao L, et al. 5′ CpG island methylation is associated with transcriptional silencing of the tumour suppressor p16/CDKN2/MTS1 in human cancers. Nat Med 1995;1:686–92.
19. Gonzalez-Zulueta M, Bender CM, Yang AS, et al. Methylation of the 5′ CpG island of the p16/CDKN2 tumor suppressor gene in normal and transformed human tissues correlates with gene silencing. Cancer Res 1995;55:4531–5.
20. Herman JG, Umar A, Polyak K, et al. Incidence and functional consequences of hMLH1 promoter hypermethylation in colorectal carcinoma. Proc Natl Acad Sci U S A 1998;95:6870–5.
21. Esteller M, Silva JM, Dominguez G, et al. Promoter hypermethylation and BRCA1 inactivation in sporadic breast and ovarian tumors. J Natl Cancer Inst 2000;92: 564–9.
22. Nass SJ, Herman JG, Gabrielson E, et al. Aberrant methylation of the estrogen receptor and E-cadherin 5′ CpG islands increases with malignant progression in human breast cancer. Cancer Res 2000;60:4346–8.
23. Rodriguez LG, Wu X, Guan JL. Wound-healing assay. Methods Mol Biol 2005;294:23–9.
24. Thiery JP. Epithelial-mesenchymal transitions in tumour progression. Nat Rev Cancer 2002;2:442–54.
25. Pampalakis G, Sotiropoulou G. Tissue kallikrein proteolytic cascade pathways in normal physiology and cancer. Biochim Biophys Acta 2007;1776:22–31.
26. Nan X, Meehan RR, Bird A. Dissection of the methyl-CpG binding domain from the chromosomal protein MeCP2. Nucleic Acids Res 1993;21:4886–92.
27. Jones PL, Veenstra GJ, Wade PA, et al. Methylated DNA and MeCP2 recruit histone deacetylase to repress transcription. Nat Genet 1998;19:187–91.
28. Eden S, Hashimshony T, Keshet I, Cedar H, Thorne AW. DNA methylation models histone acetylation. Nature 1998;394:842.
29. Nan X, Ng HH, Johnson CA, et al. Transcriptional repression by the methyl-CpG-binding protein MeCP2 involves a histone deacetylase complex. Nature 1998;393: 386–9.
30. Fuks F, Hurd PJ, Wolf D, Nan X, Bird AP, Kouzarides T. The methyl-CpG-binding protein MeCP2 links DNA methylation to histone methylation. J Biol Chem 2003; 278:4035–40.
31. Gan Y, Shen YH, Wang J, et al. Role of histone deacetylation in cell-specific expression of endothelial nitric-oxide synthase. J Biol Chem 2005;280:16467–75.
32. Shaw JL, Diamandis EP. Distribution of 15 human kallikreins in tissues and biological fluids. Clin Chem 2007;53:1423–32.
33. Ni X, Zhang W, Huang KC, et al. Characterization of human kallikrein 6/protease M expression in ovarian cancer. Br J Cancer 2004;91:725–31.
34. Oikonomopoulou K, Hansen KK, Saifeddine M, et al. Proteinase-activated receptors, targets for kallikrein signaling. J Biol Chem 2006;281:32095–112.
35. Ge L, Shenoy SK, Lefkowitz RJ, DeFea K. Constitutive protease-activated receptor-2-mediated migration of MDA-MB-231 breast cancer cells requires both β-arrestin-1 and -2. J Biol Chem 2004;53:55419–24.
36. Yang J, Mani SA, Donaher JL, et al. Twist, a master regulator of morphogenesis, plays an essential role in tumor metastasis. Cell 2004;117:927–39.
37. Cheng WF, Hung CF, Chen CA, et al. Characterization of DNA vaccines encoding the domains of calreticulin for their ability to elicit tumor-specific immunity and antiangiogenesis. Vaccine 2005;23:3864–74.
38. Buhler H, Schaller G. Transfection of keratin 18 gene in human breast cancer cells causes induction of adhesion proteins and dramatic regression of malignancy *in vitro* and *in vivo*. Mol Cancer Res 2005;3: 365–71.
39. Willipinski-Stapelfeldt B, Riethdorf S, Assmann V, et al. Changes in cytoskeletal protein composition indicative of an epithelial-mesenchymal transition in human micrometastatic and primary breast carcinoma cells. Clin Cancer Res 2005;11:8006–14.
40. Pampalakis G, Arampatzidou M, Amoutzias G, Kossida S, Sotiropoulou G. Identification and analysis of mammalian KLK6 orthologue genes for prediction of physiological substrates. Comput Biol Chem 2008;32: 111–21.
41. Lopéz-Otín C, Matrisian LM. Emerging roles of proteases in tumour suppression. Nat Rev Cancer 2007;7:800–8.
42. Palmer HG, Sanchez-Carbayo M, Ordonez-Moran P, Larriba MJ, Cordon-Cardo C, Munoz A. Genetic signatures of differentiation induced by 1α,25-dihydroxy-vitamin D3 in human colon cancer cells. Cancer Res 2003;63:7799–806.
43. Lin R, Nagai Y, Sladek R, et al. Expression profiling in squamous carcinoma cells reveals pleiotropic effects of vitamin D3 analog EB1089 signaling on cell proliferation, differentiation, and immune system regulation. Mol Endocrinol 2003;16:1243–56.